Conference Paper, Published Version

Guo, J.; Kerenyi, K.; Shan, H.; Xie, Z.; Zhai, Y.; Zhao, L.

Time-Dependent Scour Depth under Bridge-Submerged Flow

Time-Dependent Scour Depth under Bridge-Submerged Flow

J. Guo[1], K. Kerenyi[2], H. Shan[1], Z. Xie[1], Y. Zhai[1], and L. Zhao[1]

[1]Dept. of Civil Engineering, University of Nebraska-Lincoln, PKI 204D, 1110 67th ST, Omaha, NE 68182; PH (402)-554-3873; email: jguo2@unl.edu
[2]Office of Infrastructure R&D, Turner-Fairbank Highway Research Center, Federal Highway Administration, 6300 Georgetown Pike, McLean, VA 22101.

ABSTRACT

Current practice for determining the scour depth at a bridge crossing is based on the equilibrium scour depth of a design flood (e.g., 50-year, 100-year, and 500-year flood events), which is unnecessarily larger than a real maximum scour depth during a bridge life span since the peak flow period of a flood event is often much shorter than the corresponding scour equilibrium time. The objective of this study was to present a design method for time-dependent scour depth under bridge-submerged flow. To this end, a series of flume experiments on scour depth under bridge-submerged flow were conducted to collect scour data at different times. A semi-empirical model for estimating time-dependent scour depth was then presented based on the mass conservation of sediment, which agrees very well with the collected data. The proposed method can appropriately reduce the design depth of bridge scour according to design flow and a peak flow period, which can translate into significant savings in the construction of bridge foundations.

INTRODUCTION

Equilibrium scour depth under bridge-submerged flow at clear water threshold condition has been studied by Arneson and Abt (1998), Umbrell et al. (1998), Lyn (2008), and Guo et al. (2009). These studies showed that equilibrium conditions are attained under very long flow durations. In other words, the use of an equilibrium scour depth leads to overly conservative scour depth estimates that translate into excessive costs in the construction of bridge foundations. To improve the cost-efficiency of bridge foundation designs or retrofits, the time-dependent scour depth under bridge-submerged flow is of practical relevance.

The study of time-dependent scour depth has been reported extensively in literature, but all of them were under free surface flow condition about pier scour (Dargahi 1990, Yanmaz and Alitmbilek 1991, Melville 1992, Kothyari et al. 1992, Melville and Chiew 1999, Chang 2004, Oliveto and Hager 2005, Lopez et al. 2006, Yanmaz 2006, Lai et al. 2009) and abutment scour (Oliveto and Hager 2002, Coleman et al. 2003, Dey and Barbhuiya 2005, Yanmaz and Kose 2009). None of them were about general scour under bridge-submerged flow condition. The objective of this study was then to develop a semi-empirical model for computing the time-dependent variation of the maximum clear-water scour depth under bridge-submerged flow. To this end, a series of flume tests were, first, conducted to collect time-dependent scour data. A semi-empirical model was, next, developed based on the conservation of mass for sediment. The proposed model was, then, tested by the collected data. Finally, an implication and limitation was noted for guiding practical applications and further researches.

EXPERIMENTAL STUDY

The experimental study was aimed at understanding the time-dependent scour processes in bridge-submerged flow and collecting data for the development of a semi-empirical model for scour depth. The experiments were performed in the FHWA J. Sterling Jones Hydraulics Laboratory, located at the Turner-Fairbank Highway Research Center in McLean, VA. The experimental setup, results and discussion are described in the following subsections.

Experimental Setup

The experimental setup was the same as that in Guo et al. (2009). The flume had a length of 21.35 m, width of 1.83 m, and depth of 0.55 m, with clear sides and a stainless steel bottom that was about horizontal, where although a uniform flow could not be formed in the flume, it does not affect the results significantly since bridge-submerged flows are rapidly varied, the effect of bottom slopes can be neglected. In the middle of the flume was installed a test section that consists of a narrowed channel with length of 3.04 m and width of 0.63 m, a 40-cm sediment recess, and a model bridge above the recess. A honeycomb flow straightener and a trumpet-shaped inlet were carefully designed to smoothly guide the flow into the test channel. The water in the flume was supplied by a circulation system with a sump of 210 m^3 and a pump with capacity of 0.3 m^3/s; the depth of flow was controlled by a tailgate; and the experimental discharges were controlled by a LabView program and checked by an electromagnetic flowmeter.

During the experiments, two uniform sands (the gradation coefficient $\sigma_g < 1.5$) were used: a median diameter $d_{50} = 1.14$ mm with $\sigma_g = 1.45$, and a median diameter $d_{50} = 2.18$ mm with $\sigma_g = 1.35$. The previous study (Guo et al. 2009) has shown that the scour depth in submerged flow is independent of the number of girders so that only a six-girder deck was tested in this study. The deck had rails at the edges that could pass overflow on the deck surface whose elevation was adjustable, permitting the deck to have eight different inundation levels. A LabView program was used to control an automated flume carriage that was equipped with an Micro Acoustic Doppler Velocimeter (MicroADV) for records of velocities and a laser distance sensor for records of depths of flow and scour. The MicroADV (SonTek 1997) measures 3-dimensional flow in a cylindrical sampling volume of 4.5 mm in diameter and 5.6 mm in height with a small sampling volume located about 5 cm from the probe; the range of velocity measurements is from about 1 mm/s to 2.5 m/s. In this experiment, velocity measurements were taken in a horizontal plane located at a cross-section 22 cm upstream of the bridge. The LabView program was set to read the MicroADV probe and the laser distance sensor for 60 seconds at a scan rate of 25 Hz. According to the users manual, the MicroADV has an accuracy of $\pm 1\%$ of measured velocity, and the laser distance sensor has an accuracy of ± 0.2 mm.

Two discharges were applied in the experiments. They were determined

Table 1: Experimental conditions

Approach flow conditions:	$h_u = 25\,\mathrm{cm}$, $R_h = 13.9\,\mathrm{cm}$
	$V_u = 42.5\,\mathrm{cm/s}$, $d_{50} = 1.14\,\mathrm{mm}$, $\sigma_g = 1.45$, $\mathrm{Re} = 59100$, $\mathrm{Fr} = 0.271$
	$V_u = 48.2\,\mathrm{cm/s}$, $d_{50} = 2.18\,\mathrm{mm}$, $\sigma_g = 1.35$ $\mathrm{Re} = 66700$, $\mathrm{Fr} = 0.308$
Bridge opening heights:	$h_b = 13, 16$, and 19 cm
Scour measurements at:	$t = 0.5, 1, 2, 4, 8, 12, 16, 20, 24, 30, 36$, and 42 hours

Note: Re is based on hydraulic radius, and Fr based on flow depth.

by a critical velocity and the flow cross-section in the test channel. The critical velocity was preliminarily calculated by Neill's (1973) equation and adjusted by a trial and error method. The critical velocity of sediment $d_{50} = 1.14$ mm was approximately 0.425 m/s and the corresponding experimental discharge Q was 0.0669 m^3/s. The critical velocity of sediment $d_{50} = 2.18$ mm was approximately 0.482 m/s and the corresponding experimental discharge was 0.0759 m^3/s. To study the scour processes, scour morphologies at eleven times were measured for each given bridge opening height. The settings of the flow, sediment, bridge height and designated times are listed in Table 1, where the Froude and Reynolds numbers mean the approach flows were subcritical turbulent flows.

For each test with designated bright height and scour time, it was proceeded as follows: 1) Filled the sediment recess with sand and evenly distributed sand on the bottom of the flume until the depth of sand was 60 cm in the sediment recess and 20 cm in the test channel. 2) Installed a bridge deck at a designated elevation and positioned it perpendicular to the direction of flow. 3) Pumped water gradually from the sump to the flume to the experimental discharge that was controlled by the LabView. 4) Checked the approach velocity distributions in the vertical and lateral to see if they were more or less uniform away from the walls, and ran each test until the designated time. 5) Gradually emptied water and carefully removed the model bridge from the flume. 6) Scanned the 3-dimensional scour morphology using the laser distance sensor with a grid size of $5\,\mathrm{cm} \times 5\,\mathrm{cm}$.

Results and Discussion

The major results were the time-dependent variations of 3-dimensional scour morphology, which were documented in a huge MS Excel file and will be published in the web site of the FHWA Hydraulics Lab. A representation of 3-dimensional scour processes at different times is shown in Figure 1, and the corresponding width-averaged longitudinal scour profiles are shown in Figure 2. Both figures show that: (1) The shape of the scour holes remains almost unchanged as time elapses. (2) The scour hole develops rapidly from $t = 0$ to 0.5 hrs, which means the rate of change of scour depth is very large at the beginning of scour. (3) The scour depth increases as time elapses, but at $t = 30 - 42$ hrs the change of scour depth is negligible and the rate of change tends to zero, which implies that an

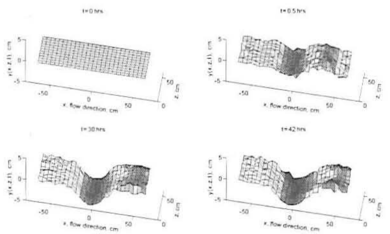

Figure 1. Scour evolution

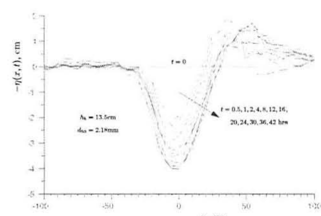

Figure 2. Width average scour profiles

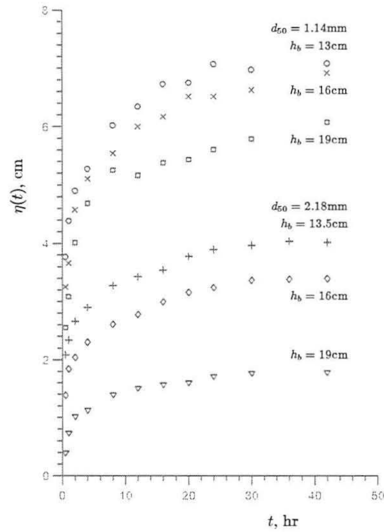

Figure 3. Maximum scour depth

equilibrium scour hole was attained approximately at $t = 30-42$ hrs. (4) The position of the maximum scour depth is close to the outlet of the bridge, at $x = -0.5$ to 0 cm, where $x = 0$ is 4 cm from the downstream face of the bridge. (5) In general, the scour morphology is approximately 2-dimensional before the maximum scour depth but 3-dimensional after the maximum scour depth.

For engineering concerns, the most important is the time-dependent variation of the maximum scour depths, which are summarized in Figure 3 that again shows as time elapses, the maximum scour depth, $\eta(t)$, increases but the rate of change decreases and tends to zero as an equilibrium scour approaches. Further discussion of the maximum scour depths is addressed in next section.

SEMI-EMPIRICAL MODEL FOR MAXIMUM SCOUR DEPTH

Scour processes are described by the conservation of mass for sediment, which is often called the Exner equation (Paola and Voller 2005). For one-dimensional flow, it is written as

$$-c_b \frac{\partial \eta}{\partial t} + \frac{\partial q_s}{\partial x} = 0 \qquad (1)$$

where c_b = bedload concentration, η = scour depth at time t (Figure 4), q_s = volumetric sediment transport rate per unit width, and x = coordinate in the flow direction. Assume that scour processes in clear water are mainly due to bedload transport, the sediment transport rate, q_s, in Eq. (1) can then be approximated

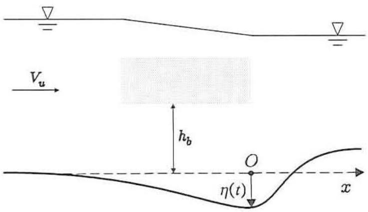

Figure 4. Definition of scour depth

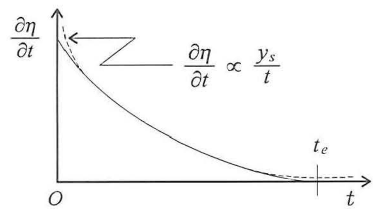

Figure 5. Sketch of scour rate

by the Meyer-Peter equation (Chien and Wan 1999, p339)

$$\frac{q_s}{\sqrt{(s-1)\,g d_{50}^3}} = 8\left(\frac{\tau_0 - \tau_c}{(s-1)\,\rho g d_{50}}\right)^{3/2} \tag{2}$$

where s = specific gravity of sediment, g = gravitational acceleration, d_{50} = diameter of sediment, $\tau_0 = \tau_0\,(x,t)$ = bed shear stress varying with location x and time t, τ_c = critical shear stress for bedload motion, and ρ = density of water.

Substituting Eq. (2) into Eq. (1) and rearranging it gives

$$\frac{\partial \eta}{\partial t} = \frac{12}{(s-1)\,c_b}\sqrt{\frac{\tau_0 - \tau_c}{\rho}}\left(\frac{1}{\rho g}\frac{\partial \tau_0}{\partial x}\right) \tag{3}$$

where

$$\tau_0 = \frac{f}{8}\rho V_b^2 \tag{4}$$

in which f = friction factor that varies with a Reynolds number and relative roughness, and V_b = cross-sectional average velocity under a bridge, which varies spatially and temporally. Eqs. (3) and (4) show that the rate of change of scour depth depends on the flow condition, $V_b\,(x,t)$, and sediment (packing density c_b, critical shear stress τ_c, and friction factor f). At the beginning, $t = 0$, of a scour process, the value of $\partial\eta/\partial t$ is large and positive since $\tau_0 > \tau_c$ and $\partial\tau_0/\partial x > 0$ (because downstream transport rate is always larger during a scour phase); after that, the value of $\partial\eta/\partial t$ decreases with time since both $\tau_0 - \tau_c$ and $\partial\tau_0/\partial x$ decrease with time; finally, the value of $\partial\eta/\partial t$ becomes zero when an equilibrium scour depth is attained. Accordingly, the rate of change of scour depth, $\partial\eta/\partial t$, can be represented by the solid line in Figure 5 where t_e = equilibrium time.

Theoretically, the solution of Eq. (3) must be coupled with a flow equation that describes the spatial and temporal variation of velocity $V_b\,(x,t)$ under a bridge. Nevertheless, the nonlinear interaction between scour depth and velocity under a bridge makes an exact solution for η impossible. For engineering concern, this analysis focuses on the temporal variation at the maximum scour depth where $x = 0$, i.e., $\eta = \eta(0,t)$. According to Figure 5, as a first approximation in the middle of a scour phase, one can hypothesize

$$\frac{\partial \eta}{\partial t} \propto \frac{y_s}{t} \tag{5}$$

where the equilibrium scour depth y_s, which is related to flow conditions and has been discussed in Guo et al. (2009), is introduced since it is an appropriate scaling length of scour depth η. Eq. (5) is represented by the dashed line in Figure but it is not valid at $t = 0$ and $t = t_e$. Eq. (5) may be rewritten as

$$\frac{\partial \eta}{\partial t} = \frac{k y_s}{t} \tag{6}$$

where the constant k reflects the effect of sediment, as suggested by c_b, τ_c and f in Eqs. (3) and (4).

Integrating Eq. (6) and rearranging it gives

$$\frac{\eta}{y_s} = k \ln t + B \tag{7}$$

where the integration constant B is approximately determined by the equilibrium condition, $\eta = y_s$ at $t = t_e$. Substituting this condition into Eq. (7) results in

$$B = 1 - k \ln t_e \tag{8}$$

Eq. (7) then becomes

$$\frac{\eta}{y_s} = k \ln \frac{t}{t_e} + 1 \tag{9}$$

which means in the middle of a scour process, the evolution of scour depth approximately follows a log law, like the law of wall in turbulent boundary layers.

Note that although the constant B in Eq. (8) is determined at $t = t_e$, Eq. (9) should not be valid at $t = 0$ and $t = t_e$ due to the hypothesis of Eq. (5), as shown in Figure 5. Fortunately, the scour depth at $t = 0$ is insignificant in practice so that one can leave this flaw alone. The second flaw at $t = t_e$ can be fixed by analogizing it to the modified log-wake law in turbulent boundary layers (Guo and Julien 2003, Guo et al. 2005), which means one can force the rate of change of scour depth to be zero at $t = t_e$ by adding a cubic function to Eq. (9)

$$\frac{\eta}{y_s} = k \left[\ln \frac{t}{t_e} - \frac{1}{3} \left(\frac{t}{t_e} \right)^3 + \frac{1}{3} \right] + 1 \tag{10}$$

where the equilibrium time t_e is characterized by the overall flow conditions and may be expressed by

$$t_e = C \frac{h_b}{V_u} \tag{11}$$

where C is an undetermined constant, h_b = bridge opening height before scour (Figure), and V_u = approach velocity. Substituting Eq. (11) into Eq. (10) gives

$$\frac{\eta}{y_s} = k \left[\ln \frac{t V_u}{C h_b} - \frac{1}{3} \left(\frac{t V_u}{C h_b} \right)^3 + \frac{1}{3} \right] + 1 \tag{12}$$

which is called the log-cubic law for time-dependent scour depth.

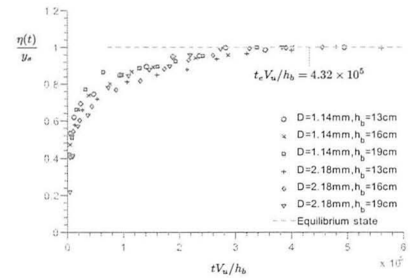

Figure 6. Test of similarity hypothesis

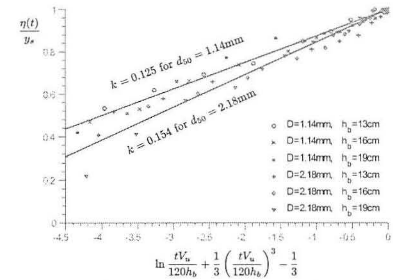

Figure 7. Determination of k values

One can summarize the above with the following hypothesis: Time-dependent scour depth may be described by a log-cubic law, Eq. (12), where the scour depth η is scaled by its equilibrium depth y_s, the time t is scaled by the approach velocity V_u and bridge opening height h_b, and the parameter k may increase with increasing sediment size while the parameter C may be a universal constant.

TEST OF SEMI-EMPIRICAL MODEL

To test the hypothesis, the present experimental data are, first, plotted according to η/y_s versus tV_u/h_b in Figure 6, which demonstrates that the scour depth η and time t are indeed appropriately scaled by y_s and h_b/V_u, respectively. The equilibrium state is, next, read from Figure 6 where

$$\frac{t_e V_u}{h_b} \approx 4.32 \times 10^5 \tag{13}$$

which gives the constant C in Eq. (11) as

$$C \approx 4.32 \times 10^5 \tag{14}$$

One can, then, clearly see from Figure 6 that most of the data points for $d_{50} = 1.14\,\text{mm}$ (blue) are above those for $d_{50} = 2.18\,\text{mm}$ (red), which just confirms the hypothesis that the value of k increases with increasing sediment size (since the value of the brackets of Eq. (12) is negative). Furthermore, using a nonlinear least-squares method in MatLab, fitting Eq. (12) to the present data gives

$$\begin{array}{ll} k = 0.125 & \text{for } d_{50} = 1.14\,\text{mm} \\ k = 0.154 & \text{for } d_{50} = 2.18\,\text{mm} \end{array} \tag{15}$$

which are shown in Figure 7 through the slopes. Finally, the model parameters in Eqs. (14) and (15) can well fit the log-cubic law, Eq. (12), to the data in Figures 8 and 9 for $d_{50} = 1.14\,\text{mm}$ and $2.18\,\text{mm}$, respectively. The corresponding correlation coefficients, R^2, and standard deviations, σ, are as follows:

$$\begin{array}{lll} R^2 = 0.982, & \sigma = 0.030, & \text{for } d_{50} = 1.14\,\text{mm} \\ R^2 = 0.963, & \sigma = 0.036, & \text{for } d_{50} = 2.18\,\text{mm} \end{array}$$

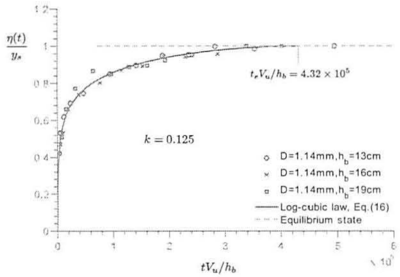

Figure 8. Test of Eq. (12) with $d_{50} = 1.14\,\mathrm{mm}$

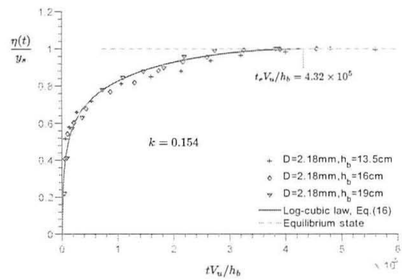

Figure 9. Test of Eq. (12) with $d_{50} = 2.18\,\mathrm{mm}$

which implies that with a 68% confidence interval, the estimated scour depth has an error of $\pm\,(3-4)\,\%$ of equilibrium depth y_s; and with a 95% confidence interval, the estimated scour depth has an error of $\pm\,(6-7)\,\%$ of equilibrium depth y_s.

One can conclude that the log-cubic law, Eq. (12), indeed describes the time-dependent scour depth under bridge-submerged flow where the parameter C is a universal constant, but the parameter k increases with increasing sediment size. Because of the limitation of sediment sizes, a general relationship between the parameter k and sediment size d_{50} cannot be generated in this study.

IMPLICATION AND LIMITATION

Current practice for determining the scour depth at a bridge crossing is based on the equilibrium scour depth of a design flood (e.g., 50-year, 100-year, and 500-year flood events), which is unnecessarily larger than a real maximum scour depth during a bridge life span since the peak flow period of a flood event is often much shorter than its equilibrium time. The proposed method can be used to estimate the evolution of scour depth at a certain time, which means it can appropriately reduce the design depth and construction cost of a bridge foundation according to design flow and a peak flow period. Nevertheless, the proposed method is limited to steady flow with clear water conditions and uniform bed materials. Its applications to unsteady flow (hygrograph) and live-bed conditions is the next step of this research in the future.

Besides, when applying Eq. (12) to practice, one has to note that: (1) the equilibrium scour depth y_s is estimated by Guo et al. (2009) although the measured values were used in the present study; and (2) the proposed method is only valid for

$$\frac{tV_u}{h_b} \leq 4.32 \times 10^5 \tag{16}$$

when $tV_u/h_b > 4.32 \times 10^5$, the equilibrium scour depth is used where $\eta = y_s$.

CONCLUSIONS

The following conclusions can be drawn from this study: (1) The shape of the longitudinal scour profiles remains almost unchanged with respected to time, shown in Figures 1 and 2. (2) The position of the maximum scour depth quickly moves to its equilibrium position that is close to the downstream edge of the bridge deck. (3) The rate of change of scour depth decreases as time elapses and tends to be zero as the scour approaches to its equilibrium state, as shown in Figure 3 by the change of slope. (4) The maximum scour depth can be described by two similarity numbers where the time-dependent scour depth is scaled by the corresponding equilibrium scour depth, and the time by the approach velocity and bridge opening height, as shown in Figure 6. (5) The time-dependent scour depth can be estimated by the log-cubic law, Eq. (12), which agrees very well with the collected flume data (Figures 8 and 9). (6) The proposed method may be used to estimate the evolution of scour depth at a certain time, which can appropriately reduce the design depth and construction cost of a bridge foundation according to design flow and a peak flow period.

ACKNOWLEDGMENTS

This study was financially supported by the FHWA Hydraulics R&D Program with Contract No. DTFH61-04-C-00037. The writers would like to thank Mr. Oscar Berrios for running a part of the tests and collecting the scour data for sediment $d_{50} = 2.18\,\text{mm}$.

REFERENCES

Arneson, L. A., and Abt, S. R. (1998). "Vertical contraction scour at bridges with water flowing under pressure conditions." *Transportation Research Record.* 1647, 10-17.

Chang, W. Y., Lai, J. S., and Yen, C. L. (2004). "Evolution of scour depth at circular bridge piers." *J. Hydraul. Res.*, 130(9), 905-913.

Chien, N., and Wan, Z. (1999). *Mechanics of Sediment Transport.* ASCE Press.

Coleman, S. E., Lauchlan, C. S., and Melville, B. W. (2003). "Clear-water scour development at bridge abutments." *J. Hydraul. Res.*, 41(5), 521-531.

Dargahi, B. (1990). "Controlling mechanism of local scouring." *J. Hydraul. Engrg.*, 116(10), 1197-1214.

Dey, S., and Barbhuiya, A. K. (2005). "Time variation of scour at abutments." *J. Hydraul. Engrg.*, 131(1), 11-23.

Guo, J., and Julien, P. Y. (2003). "Modified log-wake law for turbulent flow in smooth pipes." *J. Hydraul. Res.*, 41(5), 493-501.

Guo, J., Julien, P. Y., and Meroney, R. N. (2005). "Modified log-wake law for zero-pressure-gradient turbulent boundary layer." *J. Hydraul. Res.*, 43(4), 421-430.

Guo, J., Kerenyi, K., Pagan-Ortiz, J., and Flora, K. (2009). "Submerged-flow bridge scour under maximum clear-water conditions." Submitted to *J. Hydraul. Engrg.*

Kothyari, U. C., Garde, R. C., and Raju, K. G. R. (1992). "Temporal variation of scour around circular bridge piers." *J. Hydraul. Engrg.*, 118(8), 1091-1106.

Lai, J. S., Chang, W. Y., Yen, Y. L. (2009). "Maximum local scour depth at bridge piers under unsteady flow." *J. Hydraul. Engrg.*, 135(7), 609-614.

Lopez, G., Teixeira, L., Ortega-Sanchez, M., and Simarro, G. (2006). "Discussion: Further results to time-dependent local scour at bridge elements." *J. Hydraul. Engrg.*, 132(9), 995-996.

Lyn, D. A. (2008). "Pressure-flow scour: a re-examination of the HEC-18 equation." *J. Hydraul. Engrg.*, 134(7), 1015-1020.

Melville, B. W. (1992). "Discussion: Study of time-dependent local scour around bridge piers." *J. Hydraul. Engrg.*, 118(11), 1593-1595.

Melville, B. W., and Chiew, Y. M. (1999). "Time scale for local scour at bridge piers." *J. Hydraul. Engrg.*, 125(1), 59-65.

Oliveto, G., and Hager, W. H. (2002). "Temporal evolution of clear water pier and abutment scour." *J. Hydraul. Engrg.*, 128(9), 811-820.

Oliveto, G., and Hager, W. H. (2005. "Further results to time-dependent local scour at bridge elements." *J. Hydraul. Engrg.*, 131(2), 97-105.

Paola, C., and Voller, V. R. (2005). "A generalized Exner equation for sediment mass balance." *J. Geophys. Res.*, 110, F04014.1-F04014.8.

SonTek. (1997). *Acoustic Doppler velocimeter technical documentation, version 4.0*, SonTek, San Diego.

Yanmaz, A. M. (2006). "Temporal variation of clear water scour at cylindrical bridge piers." *Can. J. Civ. Eng.*, 33, 1098-1102.

Yanmaz, A. M., and Altmbilek, H. D. (1991). "Study of time-dependent local scour around bridge piers." *J. Hydraul. Engrg.*, 117(10), 1247-1268.

Yanmaz, A. M., and Kose, O. (2009). "A semi-empirical model for clear-water scour evolution at bridge abutments." *J. Hydraul. Res.*, 47(1), 110-118.